

The prodigious warp of NGC4013

R. Bottema, G. S. Shostak & P. C. van der Kruit

Kapteyn Astronomical Institute, PO Box 800,
9700 AV Groningen, The Netherlands

Non-planar distortions, or warps, in the outer gas layers of galaxies are more the rule than the exception, although the degree of warping may differ drastically from one galaxy to another¹⁻³. H I radio synthesis observations reveal that the edge-on Sbc⁴ galaxy NGC4013 has the largest regular H I warp so far observed. It extends to a large height above the plane of the galaxy, and begins abruptly at just the radius where photometry indicates the end of the luminous disk. Furthermore, at precisely this position, the rotational velocity is seen to drop by 25 km s⁻¹. These observations can only be explained by a situation in which not only the disk-light distribution, but also the disk-mass distribution, suddenly approach zero at the radius of the warp onset. On the basis of a modelling of the H I gas distribution, we conclude that our line of sight to NGC4013 is, by coincidence, one which shows the warp most clearly.

NGC4013 was observed for 2 × 12 hours with the Westerbork Synthesis Radio Telescope in June, 1982. The synthesized beam was 14.0 × 19.7 arc s full width at half maximum (FWHM) with a velocity resolution of 33.2 km s⁻¹. The total measured flux was 39.1 Jy km s⁻¹, implying a total H I mass of 1.1 × 10⁹ solar masses. All channel maps were smoothed to a resolution of 30 × 30 arc s to increase the signal-to-noise ratio, especially in the warped region. A distance of 12 Mpc has been assumed.

The smoothed total H I distribution is given in Fig. 1 and the result after integration of the data cube in the direction perpendicular to a position angle of 50° 'strip' l, v , or longitude-velocity diagram, made by integrating emission along the minor axis is shown in Fig. 2. This position angle is a good compromise between that of the outer H I distribution and the disk. It is clear from Figs 1 and 2 that the outer gas layers of NGC4013 are highly warped. Also, as can be seen from the $l-v$ diagram, the rotational velocities on both sides of the galaxy are lower in the warped region than in the disk. To unravel the morphology and kinematics in an unambiguous way, it was necessary to model the gas layer of NGC4013.

The presently fashionable model for warped galaxies is the so-called 'tilted ring model'¹. The disk and warp are divided up into a number of concentric rings of differing orientations. We

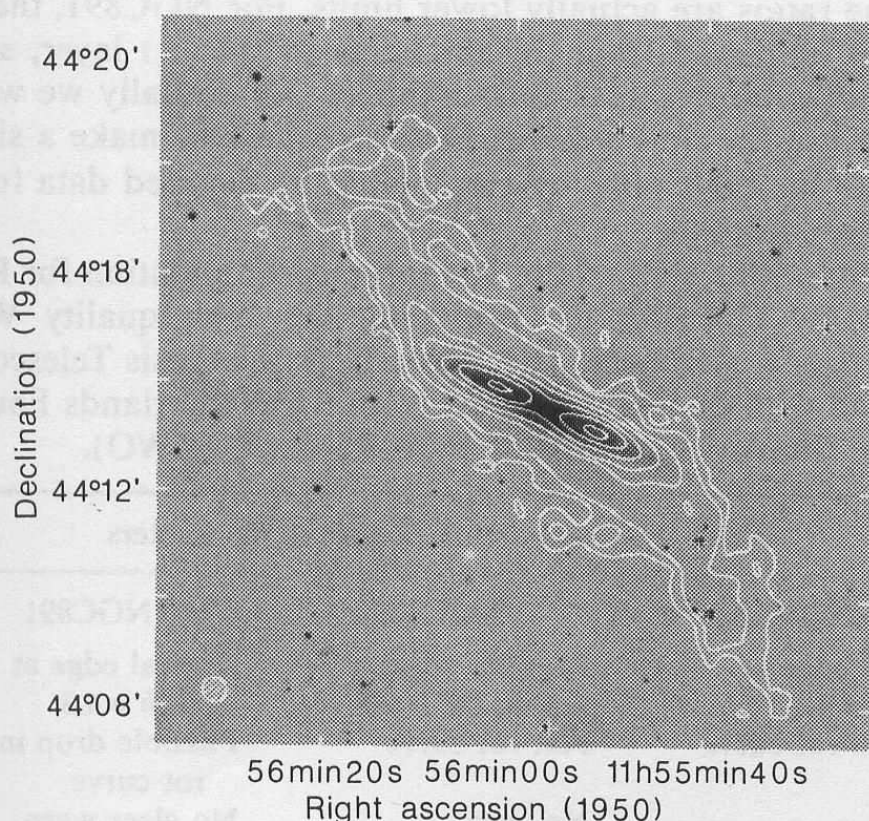


Fig. 1 The total H I distribution of NGC4013 superposed on an optical photograph in the F-band. The beamsize is 30 × 30 arc s. Contour levels are at 1.7×10^{19} , 1.1×10^{20} , 5.6×10^{20} , 1.1×10^{21} , 2×10^{21} , 2.9×10^{21} and 3.8×10^{21} H-atoms cm⁻².

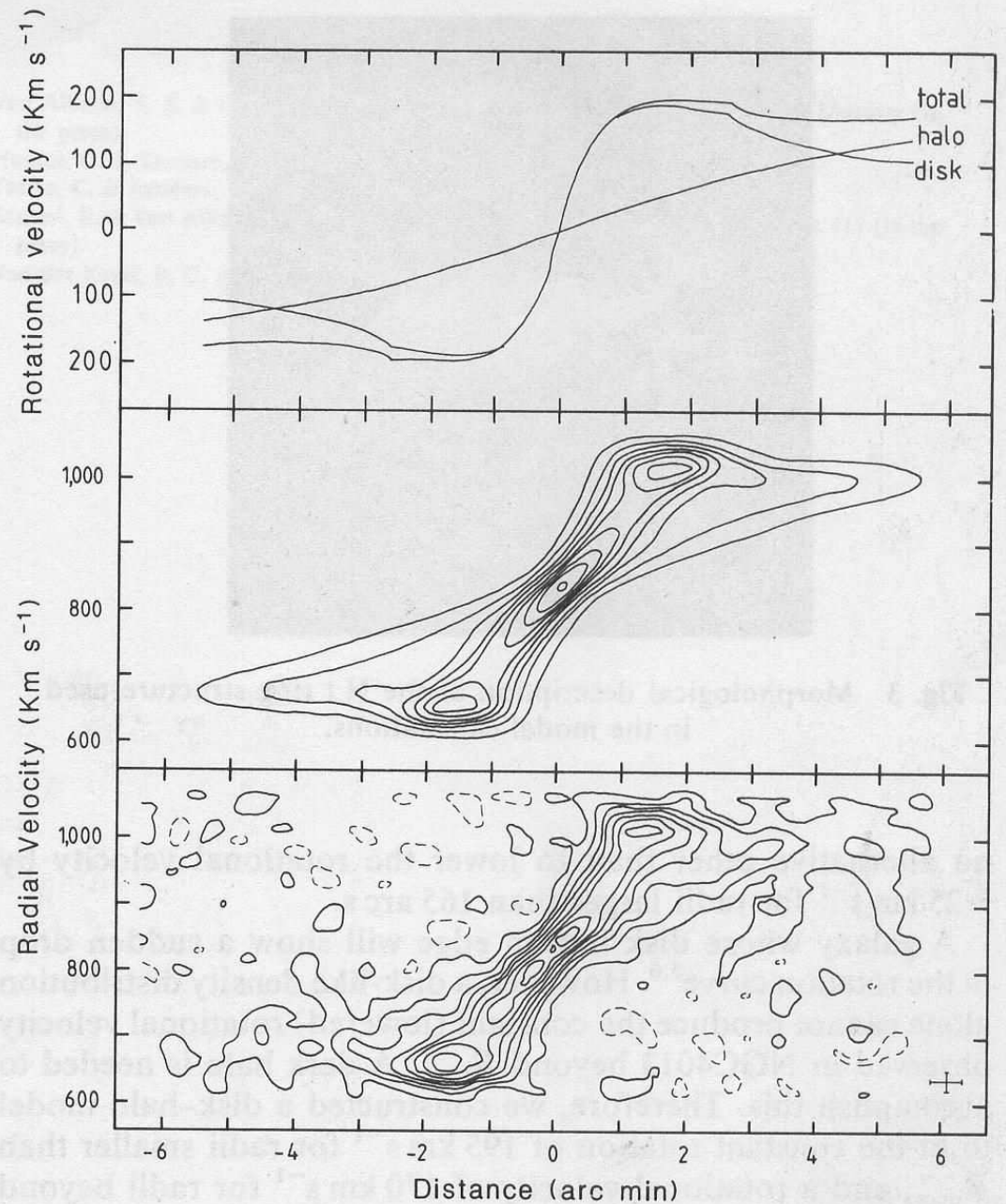


Fig. 2 Bottom: Observed $l-v$ diagram. This diagram is obtained after integration perpendicular to a position angle of 50° (major axis position angle = 66°) over the extent of the H I emission. This position angle was chosen to minimize the contribution of noise. Levels range from -8.4 K to 104 K in steps of ~14 K. Middle: Resulting $l-v$ diagram after modelling. Top: Rotation curves obtained after fitting a disk-halo mass model to the data. The 'total' rotation curve is used in the modelling.

have used this model, but have restricted the warped rings to intersect the central disk along the same line (see Fig. 3). For the present exactly edge-on galaxy, the warp can then be described with three parameters: first, the 'warp angle' α , which is the angle between the plane of the central disk and the line through the extrema (lying 1/4 circle from the line of intersection) of the concentric rings. In other words, if $\alpha = 0$, there is no warp. Second, the angle ψ , which is the angle between the line perpendicular to the line of intersection and the line of sight. For $\psi = 90^\circ$, the warp, whose maximum is then in the plane of the sky, shows up very clearly; for $\psi = 0$, it is probably only visible as a diffuse thick H I disk. The third parameter is, naturally, the radius at which the warp starts. One must, of course, also specify the surface density, thickness, rotational velocity and velocity dispersion of each ring.

To compare the ring model with our data, an exact simulation of the process of H I line observations was made. First, all the modelled line channels were calculated and smoothed in both of the two spatial directions and in velocity to match the resolution of the observations. Next, the smoothed channel set, or data cube, was integrated in velocity to get the total H I map, and then integrated in the direction perpendicular to the plane of the galaxy to obtain the $l-v$ diagram. Both the total H I map and $l-v$ diagram can be compared with the observations, and if the kinematic and structural parameters are chosen correctly, these should fit the data simultaneously.

Our first modelling effort was to try and match the observations by assuming a constant rotational velocity, and varying the angles α and ψ . This turned out to be impossible for any choice of parameters. To 'lower' the observed velocities in the outer region, ψ had to be so small that the model total H I map entirely failed to agree with the observations. Thus, there was

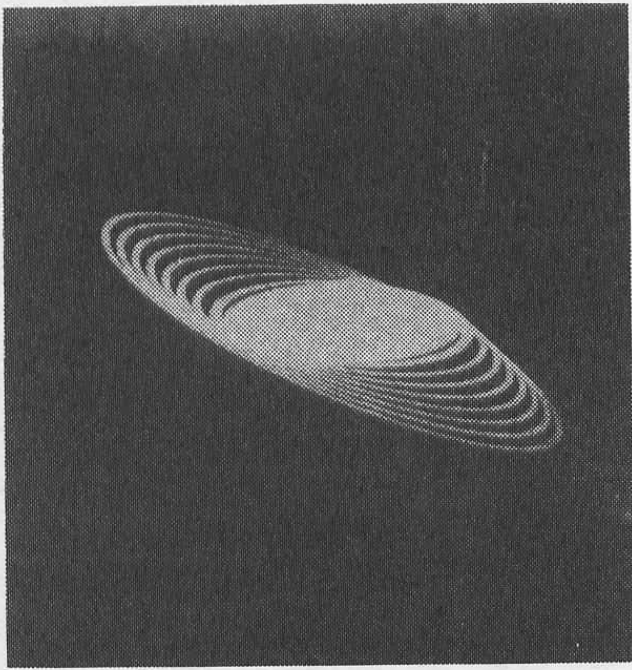


Fig. 3 Morphological description of the H I ring structure used in the model calculations.

no alternative other than to lower the rotational velocity by $\sim 25 \text{ km s}^{-1}$ for radii larger than 165 arc s.

A galaxy whose disk has an edge will show a sudden drop in the rotation curve^{5,6}. However, a disk-like density distribution alone cannot produce the constant (lowered) rotational velocity observed in NGC4013 beyond R_{max} . A dark halo is needed to accomplish this. Therefore, we constructed a disk-halo model to fit the constant rotation of 195 km s^{-1} for radii smaller than R_{max} , and a rotational velocity of 170 km s^{-1} for radii beyond R_{max} . For the disk we assumed the following distributions^{6,7}:

$$\rho = \rho_0 e^{-R/h} \text{sech}^2(z/z_0) \quad \text{for } R < R_{\text{max}} \quad (1)$$

$$= 0 \quad \text{for } R > R_{\text{max}}$$

For the halo, we have used an isothermal sphere. Adopting the maximum disk hypothesis⁸ the observed rotation curve can be obtained for a total disk mass of $5 \times 10^{10} M_{\odot}$ $M_{\text{halo}}/M_{\text{disk}} = 0.3$ for $R < R_{\text{max}}$, and a core radius for the halo of 15 kpc. This means that $M_{\text{halo}}/M_{\text{disk}} = 1.8$ for $R < 20$ kpc, the largest radius out to which the rotational velocity can be accurately derived. The corresponding rotation curve is plotted in Fig. 2, which was used as input for the channel map modelling.

In Fig. 4 we show the resulting total H I maps for three models with different values of ψ . For every model we have tried to optimize the agreement with the observations by adjusting α . Examining Fig. 4 one can see that a value of $\psi = 70^\circ$ might just fit the observations, but that $\psi = 90^\circ$ is better. This means that we just happen to be situated along the right line of sight to see the warp so clearly. The $l-v$ diagrams corresponding to the three models differ only slightly, so we only show the result for $\psi = 90^\circ$ in Fig. 2. An interesting point is that the warp starts precisely at the radius (9.5 kpc) where the rotation curve drops and the stellar disk ends. For all simulations a constant thickness of 1.3 kpc width at half-maximum density (HPW) and a velocity dispersion of 10 km s^{-1} were used for the hydrogen layer, but the conclusions are not sensitive to these assumptions.

The origin of warps is still not clearly established. One explanation is that the once regular H I disk has been distorted by tidal forces resulting from the interaction with another galaxy⁹. In the present instance, a good candidate for such a model would be NGC3938, which has almost the same redshift as NGC4013. The distance between the two galaxies is 200 kpc. Another possible explanation is that the warp is the result of a recent infall of gas from outside the galaxy.

A large warp cannot persist for more than a few rotation periods in the presence of a disk-like potential alone¹⁰. If a spherical or halo potential is added, the warp will last much longer. The very abrupt onset of the warp in this galaxy therefore indicates that at $R = R_{\text{max}}$ there is a sudden change from a disk-like to a more spherical potential. This is additionally supported by the fact that at this radius both the light and the rotational velocity suddenly drop.

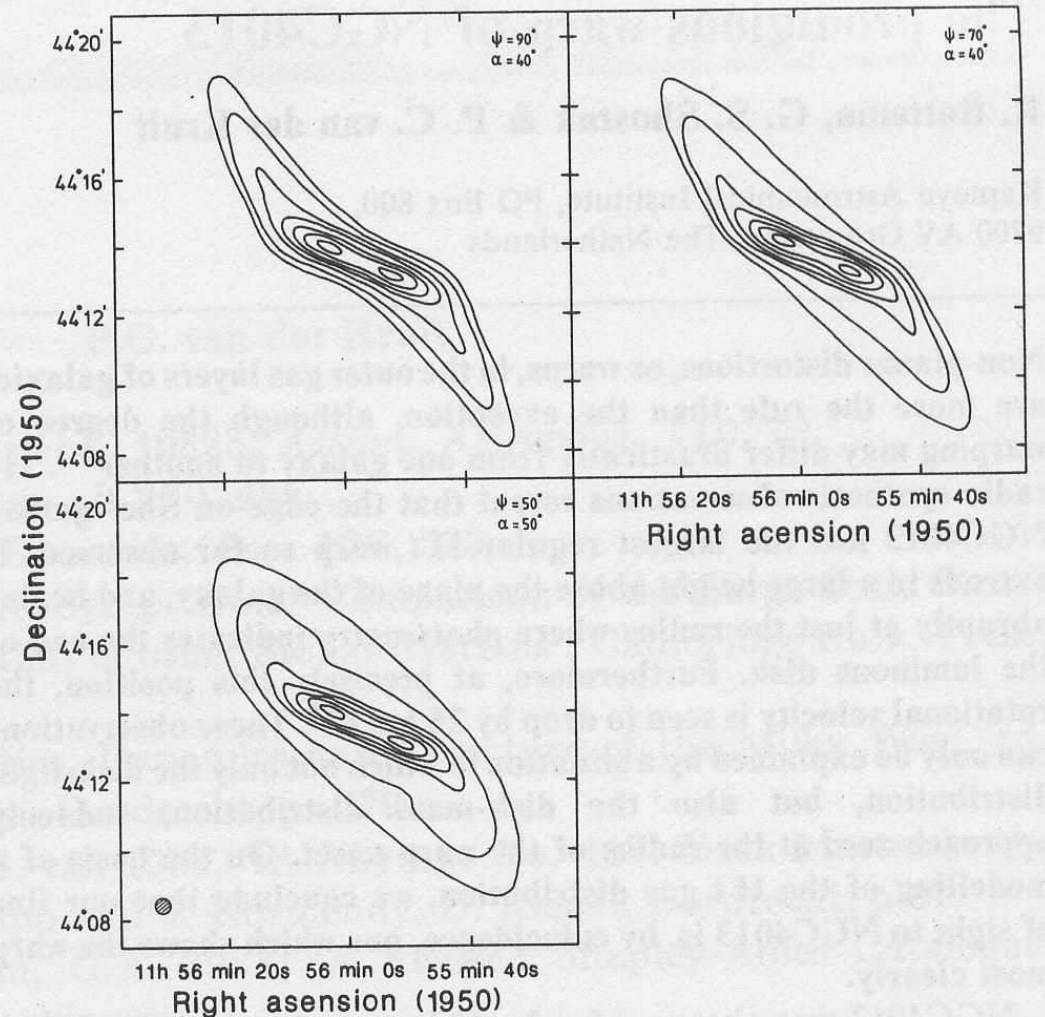


Fig. 4 Resulting total H I maps for three models. The angles α and ψ are described in the text. From comparison with the observed total H I, we conclude that $\psi > 70^\circ$.

It is instructive to compare this galaxy with galaxies of similar morphological type and dimensions to see if the large warp can be related to other galactic properties. In Table 1 we give parameters of NGC4013 together with those of the well-studied regular spiral NGC3198 and the edge-on galaxy NGC891.

The first three items in Table 1 might be related. For $R_{\text{max}}/h \sim 4$ a drop in the rotation curve should be measurable, but for $R_{\text{max}}/h \sim 5$ the drop has almost completely disappeared⁵. So the difference in rotation curve between NGC4013 and NGC3198 (drop versus flat) can be related to the fact that the disk of NGC3198 is relatively larger. Additionally, a larger disk could be responsible for damping out the warp.

In NGC3198 there is no clear evidence for the 'truncation feature' in the rotation curve around R_{max} , while there is some evidence for this in NGC891 on the south-west side¹¹. The major difference between NGC4013 and the other two galaxies is in the halo-disk mass ratio within R_{max} . For NGC4013 and NGC3198, these ratios have been derived from an analysis of the rotation curve using the maximum disk solution, and therefore the ratios are actually lower limits. For NGC891, the disk mass is estimated from the thickness of the H I layer, and is therefore a more direct measurement¹². Eventually we will be able to use the observations presented here to make a similar estimate for NGC4013 by employing the detailed data for the inner gaseous disk.

We thank the staff of the Netherlands Foundation for Radio Astronomy (NFRA) for providing the high quality WSRT observations used here. The Westerbork Synthesis Telescope is operated with financial support from the Netherlands Foundation for the Advancement of Pure Research (ZWO).

Table 1 Comparison of galaxy parameters

| NGC4013 | NGC3198 | NGC891 |
|--|--|--|
| Optical edge at $R/h = 4.1$ | Possible edge near $R/h \sim 5$ | Optical edge at $R/h = 4.3$ |
| Drop in rot curve | Flat rot curve | Possible drop in rot curve |
| Warp | No warp | No clear warp |
| $M_{\text{halo}}/M_{\text{disk}} = 0.3$ | $M_{\text{halo}}/M_{\text{disk}} = 0.8$ | $M_{\text{halo}}/M_{\text{disk}} = 2.0$ |
| at $R = R_{\text{max}} = 4.1 h$ | at $R = 4.1 h$ | at $R = R_{\text{max}} = 4.3 h$ |
| $h = 2.3 \text{ kpc}$ | $h = 2.7 \text{ kpc}$ | $h = 4.9 \text{ kpc}$ |
| $V_{\text{max}} = 195 \text{ km s}^{-1}$ | $V_{\text{max}} = 150 \text{ km s}^{-1}$ | $V_{\text{max}} = 225 \text{ km s}^{-1}$ |

Received 16 April; accepted 8 May 1987.

1. Rogstad, D. H., Lockhart, I. A. & Wright, M. C. H. *Astrophys. J.* **193**, 309 (1974).
2. Rogstad, D. H., Wright, M. C. H. & Lockhart, I. A. *Astrophys. J.* **204**, 703 (1976).
3. Sancisi, R. *Astr. Astrophys.* **53**, 159 (1976).
4. Sandage, A. & Tammann, G. A. *A Revised Shapley-Ames Catalog of Bright Galaxies* (Carnegie Inst. of Washington, Washington DC, 1981).
5. Casertano, S. *Mon. Not. R. Astr. Soc.* **203**, 735 (1983).
6. Van der Kruit, P. C. & Searle, L. *Astr. Astrophys.* **110**, 61 (1982).
7. Van der Kruit, P. C. & Searle, L. *Astr. Astrophys.* **95**, 105 (1981).
8. Van Albada, T. S. & Sancisi, R. in *Proc. of Meet. on Material Content of the Universe* (in the press).
9. Hunter, C. & Toomre, A. *Astrophys. J.* **155**, 747 (1969).
10. Tubbs, C. & Sanders, R. H. *Astrophys. J.* **230**, 736 (1979).
11. Sancisi, R. & van Albada, T. S. in *Dark Matter in the Universe, IAU Symp. No. 117* (in the press).
12. Van der Kruit, P. C. *Astr. Astrophys.* **99**, 298 (1981).

Abstract

Summary

Abstract

Summary

The present study is based on the analysis of the radial profiles of the surface brightness and the surface density of the stars in the disks of spiral galaxies. The profiles are compared with the profiles of the total light and the profiles of the dark matter. The profiles of the total light and the profiles of the dark matter are compared with the profiles of the total light and the profiles of the dark matter. The profiles of the total light and the profiles of the dark matter are compared with the profiles of the total light and the profiles of the dark matter.

The present study is based on the analysis of the radial profiles of the surface brightness and the surface density of the stars in the disks of spiral galaxies. The profiles are compared with the profiles of the total light and the profiles of the dark matter. The profiles of the total light and the profiles of the dark matter are compared with the profiles of the total light and the profiles of the dark matter. The profiles of the total light and the profiles of the dark matter are compared with the profiles of the total light and the profiles of the dark matter.

The profiles of the total light and the profiles of the dark matter are compared with the profiles of the total light and the profiles of the dark matter. The profiles of the total light and the profiles of the dark matter are compared with the profiles of the total light and the profiles of the dark matter. The profiles of the total light and the profiles of the dark matter are compared with the profiles of the total light and the profiles of the dark matter.

The profiles of the total light and the profiles of the dark matter are compared with the profiles of the total light and the profiles of the dark matter. The profiles of the total light and the profiles of the dark matter are compared with the profiles of the total light and the profiles of the dark matter. The profiles of the total light and the profiles of the dark matter are compared with the profiles of the total light and the profiles of the dark matter.

The profiles of the total light and the profiles of the dark matter are compared with the profiles of the total light and the profiles of the dark matter. The profiles of the total light and the profiles of the dark matter are compared with the profiles of the total light and the profiles of the dark matter. The profiles of the total light and the profiles of the dark matter are compared with the profiles of the total light and the profiles of the dark matter.

The profiles of the total light and the profiles of the dark matter are compared with the profiles of the total light and the profiles of the dark matter. The profiles of the total light and the profiles of the dark matter are compared with the profiles of the total light and the profiles of the dark matter. The profiles of the total light and the profiles of the dark matter are compared with the profiles of the total light and the profiles of the dark matter.

The profiles of the total light and the profiles of the dark matter are compared with the profiles of the total light and the profiles of the dark matter. The profiles of the total light and the profiles of the dark matter are compared with the profiles of the total light and the profiles of the dark matter. The profiles of the total light and the profiles of the dark matter are compared with the profiles of the total light and the profiles of the dark matter.

The profiles of the total light and the profiles of the dark matter are compared with the profiles of the total light and the profiles of the dark matter. The profiles of the total light and the profiles of the dark matter are compared with the profiles of the total light and the profiles of the dark matter. The profiles of the total light and the profiles of the dark matter are compared with the profiles of the total light and the profiles of the dark matter.